From Chiral Vibration to Static Chirality in ^{135}Nd

S. Mukhopadhyay,[1,2] D. Almehed,[1] U. Garg,[1] S. Frauendorf,[1] T. Li,[1] P. V. Madhusudhana Rao,[1] X. Wang,[1,3] S. S. Ghugre,[2] M. P. Carpenter,[3] S. Gros,[3] A. Hecht,[3,4] R. V. F. Janssens,[3] F. G. Kondev,[5] T. Lauritsen,[3] D. Seweryniak,[3] and S. Zhu[3]

[1]*Physics Department, University of Notre Dame, Notre Dame, Indiana 46556, USA*
[2]*UGC-DAE Consortium for Scientific Research, Kolkata Centre, Kolkata 700098, India*
[3]*Physics Division, Argonne National Laboratory, Argonne, Illinois 60439, USA*
[4]*Department of Chemistry and Biochemistry, University of Maryland, College Park, Maryland 20742, USA*
[5]*Nuclear Engineering Division, Argonne National Laboratory, Argonne, Illinois 60439, USA*

(Received 26 June 2007; published 23 October 2007)

Electromagnetic transition probabilities have been measured for the intraband and interband transitions in the two sequences in the nucleus ^{135}Nd that were previously identified as a composite chiral pair of rotational bands. The chiral character of the bands is affirmed and it is shown that their behavior is associated with a transition from a vibrational into a static chiral regime.

DOI: 10.1103/PhysRevLett.99.172501 PACS numbers: 21.10.Tg, 11.30.Rd, 21.60.Ev, 27.60.+j

Chirality is a well-known phenomenon in chemistry and biology as a geometric property of many molecules, in particular of complex biomolecules. Particle physics is another domain of chirality, where it describes a kinematical feature of massless particles. Both in chemistry and particle physics, space inversion changes left-handed into right-handed systems. Nuclei have been considered as achiral, because their shapes are, generally, too simple. However, it was pointed out some time ago that a triaxial nucleus becomes chiral if it rotates about an axis that lies outside the three planes spanned by the principal axes of its triaxial ellipsoidal shape [1,2]. The short, intermediate, and long axes form a screw with respect to the angular momentum vector. In contrast with molecules and massless particles, space inversion leaves nuclear chirality unchanged. The left-handed configuration is converted into the right-handed one by the time reversal operation, which changes the sign of all linear and angular momenta. Since both chiral structures have the same energy and are related by time reversal, one expects to observe two identical bands of the same parity. A number of pairs of bands have been identified in nuclei in the $A \sim 130$ and $A \sim 100$ regions of the nuclear chart and have been suggested as candidates for chiral partners [3–11]. A small observed energy difference between the states of the same spin, I, in the chiral partners indicates rapid conversion between the left-handed and right-handed configurations (chiral vibration). With decreasing energy splitting between the partner bands, the left-right mode changes from soft chiral vibration to tunneling between well-established chiral configurations (static chirality).

In addition to close level energies, the two chiral partners should deexcite in a very similar way via electromagnetic radiation. Thus, in this context, a measurement of $E2$ transition probabilities is an essential probe of nuclear chirality. Only two lifetime measurements have been published so far. For ^{128}Cs [12], it was established that the electromagnetic transition probabilities are similar, but the excitation energies of the two partner bands never approach each other. In ^{134}Pr, the two bands come very close around spin 14; however, the intraband $B(E2)$ values were found to differ by about a factor of 2 [13,14]. The latter observation was interpreted as suggesting that the change in orientation of the angular momentum vector must be accompanied by a change in shape [13], or even that the results rendered the chiral interpretation itself doubtful [14].

The study of magnetic rotation [1] suggests that chirality is better developed if the nonplanar geometry is generated by three excited quasiparticles (instead of two, as in the case of ^{134}Pr and ^{128}Cs). Such a case was realized in the nucleus ^{135}Nd, where two partner bands consistent with chirality have been observed [8]. This expectation is now borne out by the measurements and calculations presented below as the electromagnetic transition rates in the chiral bands of ^{135}Nd were found to be nearly identical. For the first time, the splitting between the chiral partners is calculated in a microscopic way by extending the tilted-axis-cranking model (TAC) by the random phase approximation (RPA). The observed transition probabilities and energies are in very good agreement with the calculations, which indicate, furthermore, that a transition from chiral vibration to static chirality occurs with increasing spin.

The experiment was carried out at the ATLAS accelerator facility at the Argonne National Laboratory, and employed a 175-MeV ^{40}Ar beam to populate high-spin states of ^{135}Nd with the ^{100}Mo(^{40}Ar, $5n$) reaction. The target was a 1.14 mg/cm^2-thick, isotopically enriched, ^{100}Mo foil backed by a 17.9 mg/cm^2-thick layer of Pb in order to slow down and stop the recoiling nuclei. A total of about 2.5×10^9 fivefold and higher-fold coincidence events were accumulated using the Gammasphere array [15]. The level scheme of ^{135}Nd is already well-established [16,17] and the chiral bands were presented in Ref. [8]; in the remainder of this Letter we refer to the partial level scheme presented therein.

For the analysis of these thick-target data with the Doppler-shift attenuation method (DSAM), the power of the BLUE database approach [18] has been employed to efficiently sort the data angle-by-angle. After building the database for each fold, and performing appropriate background subtraction [19], double-gated coincidence spectra were obtained for each ring (angle) of Gammasphere for further analysis of the relevant Doppler shifts. In the cases where the gating transition was not fully stopped, the gate was made sufficiently wide to ensure that the full peak shape was included in the gate; this eliminated a possible bias in the analysis that could be introduced by omitting part of a peak's line shape, thereby favoring a specific time component of the gating transition.

Lifetimes of states in both chiral bands were extracted using the LINESHAPE analysis codes of Wells and Johnson [20]. In each case, a total of 5000 Monte Carlo simulations of the velocity history of the recoiling nuclei traversing the target and the backing material were generated in time steps of 0.002 ps. Electronic stopping powers were calculated with the code SRIM [21]. More details about the fitting procedures can be found in Refs. [22,23].

The lifetimes of the levels with spins, I, from $29/2^-$ to $43/2^-$ in Band A, and from $31/2^-$ to $39/2^-$ in Band B, have been deduced in this work. Representative examples of DSAM fits are displayed in Fig. 1, and the extracted lifetimes are listed in Table I. Uncertainties in the lifetimes were determined from the behavior of the χ^2-fit in the vicinity of the minimum [22–24].

Reduced transition probabilities, $B(M1)$ and $B(E2)$, were derived from the resulting lifetimes and are presented in Table I and in Figs. 2 and 3. Within the experimental uncertainties, the $B(E2)$ and $B(M1)$ values for the intraband transitions of the two bands are essentially the same, pointing to their identical nature. In addition, the $B(M1)$ values of the intraband transitions exhibit a characteristic staggering with increasing spin. A similar staggering, but opposite in phase, is observed in the $B(M1)$ values of the interband transitions. All these results are fully compatible with a pure chiral interpretation of these bands [2,25].

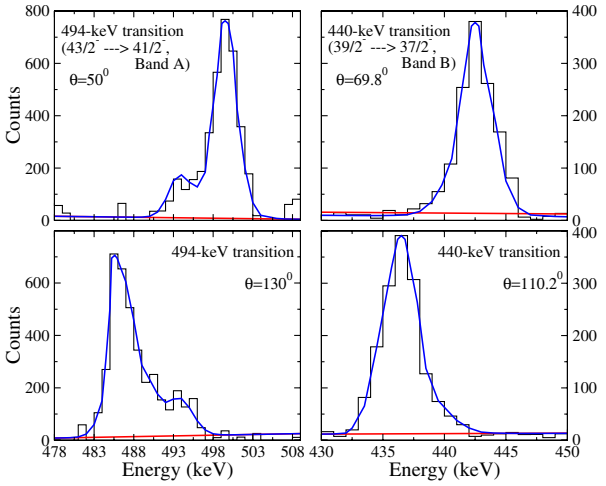

FIG. 1 (color online). Line shape fits for representative γ transitions in the chiral bands of ^{135}Nd. Left: the 494-keV transition in Band A. Right: the 440-keV transition in Band B.

We have performed new calculations for the twin bands in ^{135}Nd in the framework of TAC complemented by RPA. As proposed in Ref. [8], these bands are built on the $\{\pi h_{11/2}^2, \nu h_{11/2}\}$ configuration. TAC is a microscopic mean field method that has been shown to describe the energy and the inband transition rates of the lower of the two chiral partner bands very well (see, e.g., Refs. [5,11,26]). However, to describe the energy splitting between the two partner bands, one needs to go beyond the mean field approach. This has previously been done only in either the two-particle-plus-rotor model [2,27] or the core-quasiparticle-coupling model [28]. But, these models cannot be applied to the three-quasiparticle configuration of ^{135}Nd. Moreover, both these approaches assume that the moments of inertia are of the irrotational-flow type, which is not consistent with microscopic cranking calculations [13]. RPA, as a microscopic approach, does not have these restrictions since it describes the excitations of the equilibrium mean field as harmonic vibrations.

We use the self-consistent TAC with the QQ-force and a constant pair gap (named PQTAC in Ref. [29]) in two major N shells (4 and 5):

$$H' = h_0 + \sum_{\mu,N} \frac{\kappa_N}{2} Q_\mu^{(N)} Q_\mu^{(N)} (-)^\mu - \Delta(P^+ + P) - \vec{\omega} \cdot \vec{J} \tag{1}$$

where h_0 is the spherical Woods-Saxon energy [26] and

TABLE I. Derived lifetimes and electromagnetic transition probabilities in the chiral bands of ^{135}Nd.

Spin I [$\hbar$]	Lifetime [ps]	$B(M1)$ [μ_n^2]	$B(E2)$ [e^2b^2]
		Band A	
$\frac{29}{2}^-$	1.00(5)	3.2(2)	0.32(2)
$\frac{31}{2}^-$	0.75(8)	2.5(3)	0.32(3)
$\frac{33}{2}^-$	0.44(2)	2.2(2)	0.32(3)
$\frac{35}{2}^-$	0.28(2)	2.4(3)	0.32(3)
$\frac{37}{2}^-$	0.23(2)	1.7(3)	0.32(4)
$\frac{39}{2}^-$	0.22(2)	2.1(3)	0.13(3)
$\frac{41}{2}^-$	0.18(2)	2.1(3)	0.19(3)
$\frac{43}{2}^-$	0.16(2)	2.0(3)	0.21(4)
		Band B	
$\frac{31}{2}^-$	1.46(2)	2.7(3)	0.28(3)
$\frac{33}{2}^-$	0.87(6)	2.1(2)	0.28(3)
$\frac{35}{2}^-$	0.64(5)	2.2(2)	0.28(4)
$\frac{37}{2}^-$	0.48(3)	1.7(2)	0.29(4)
$\frac{39}{2}^-$	0.24(4)	1.9(3)	0.11(3)

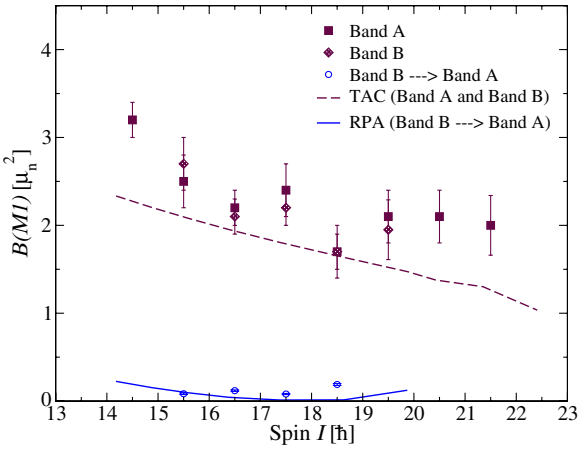

FIG. 2 (color online). Evolution of the $B(M1)$ transition rates with spin for the two chiral partner bands in ^{135}Nd. A comparison with the calculations described in the text is shown as well.

$Q_\mu^{(N)}$ are the five quadrupole operators for each N shell with an N-dependent force strength [30]:

$$\kappa_N = \kappa_0 \frac{N_L - B}{N - B}\left(\frac{2Z(N)}{A}\right)^{1/3}. \quad (2)$$

Here, $N_L = 4$ and the parameters κ_0 and $B(= 0.5)$ are chosen to reproduce the Strutinsky potential energy surface. The rotational frequency in the cranking term $\vec{\omega} \cdot \vec{J}$ is defined as $\omega_1 = \omega \sin\vartheta \cos\varphi$, $\omega_2 = \omega \sin\vartheta \sin\varphi$, and $\omega_3 = \omega \cos\vartheta$, where ϑ and φ are the two tilt angles defined in Ref. [26]. We use a proton (neutron) pairing gap $\Delta_{n,p}$ that is 50% (80%) of the odd-even mass difference. Since the proton configuration corresponds to a particle-hole excitation of the even-even system, we have used a smaller pairing gap than that of an odd-neutron system.

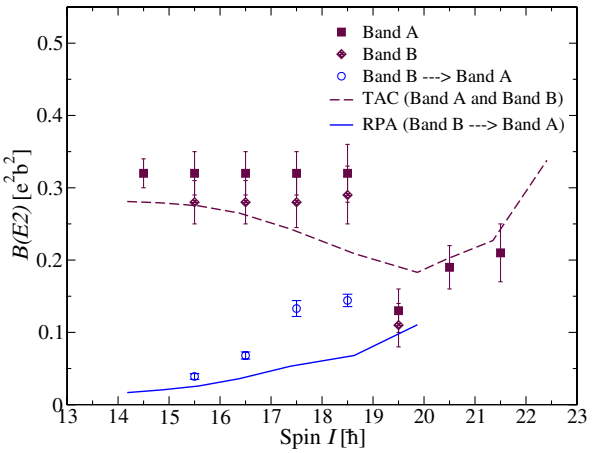

FIG. 3 (color online). Variation of the $B(E2)$ transition rates with spin for the two chiral partner bands in ^{135}Nd, together with the results of the calculations described in the text.

The RPA calculates the harmonic excitations around the mean field minimum. This chiral vibrational regime applies well below the transition point to chiral rotation, where the RPA solution goes to zero energy and the tilted mean field gets a nonzero φ value. We solved the RPA equations:

$$[H_{\mathrm{RPA}}, O_\lambda^+] = E_{\mathrm{RPA}} O_\lambda^+ \quad (3)$$

where H_{RPA} is the Hamiltonian in RPA order [31] derived from the corresponding self-consistent mean field wave function, and O_λ^+ are the RPA eigenmode operators. H_{RPA} describes the orientation, shape, and two quasiparticle degrees of freedom in the harmonic approximation. The RPA phonon energy gives the energy splitting between the zero-phonon lower band and the one-phonon excited band, and the RPA wave functions give the interband transition rates. Since RPA describes harmonic vibrations around the equilibrium, it does not contribute to the expectation values of the operators; i.e., the intraband transition rates remain the same as those given by the TAC model. Details of the RPA calculations will be provided in a future publication [32].

The TAC results reproduce the rotational energies of the bands rather well, as can be seen in Fig. 4, and the one-phonon energy matches the energy splitting between the two bands.

The angular momentum where the RPA energy goes to zero and static chirality emerges in the TAC calculations is one unit higher than the point at which the two bands come closest in the data. This coming together of the two bands has been interpreted as the onset of chiral rotation [8]. By analyzing the RPA wave functions, we can determine that the lowest phonon is dominated by fluctuations in the orientation of the shape relative to the angular momentum

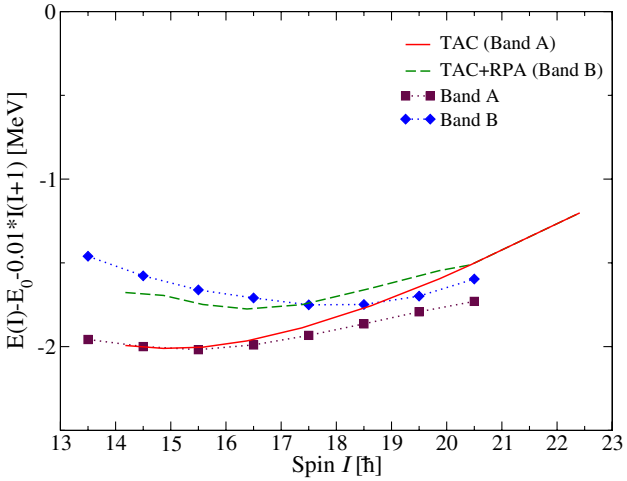

FIG. 4 (color online). Comparison, as a function of spin, of the measured and calculated energies, relative to the band head, E_0, of the chiral bands, with a rotor reference subtracted.

vector, with a small admixture of γ vibration. Details of this analysis also will be published in Ref. [32].

The calculated intraband and interband transition probabilities are also displayed in Figs. 2 and 3, respectively. There is a good agreement with the data. Below the critical frequency, the TAC calculations give $\varphi = 0$ and a slow increase of ϑ, resulting in a slowly decreasing intraband $B(E2)$. After the critical frequency, the rapid increase of φ causes the steep rise in the $B(E2)$. The calculated interband $B(E2)$'s are somewhat smaller than the observed values but exhibit the correct functional form. In accordance with the experiment, the calculated interband $B(M1)$ rates are much smaller than the intraband $B(M1)$'s; so the observed different behavior with spin is not of much consequence. Thus, the calculations reproduce the data rather well, even close to the point of transition to static chirality where the TAC + RPA approach breaks down.

The nucleus ^{135}Nd (3 quasiparticles) differs from ^{134}Pr (2 quasiparticles) by the additional $h_{11/2}$ quasiproton. The $B(E2)$ values within the two bands are about the same, as long as the chiral vibration remains near harmonic. As will be shown in a forthcoming paper [32], they may differ substantially near the instability point, where strong anharmonicities make the average tilt-angle, ϑ, different in the two bands. The resulting difference in the $B(E2)$ values is most pronounced near $\vartheta = 45°$, where the $B(E2)$'s go to zero. As compared to ^{134}Pr, the longer proton angular momentum in ^{135}Nd delays the instability; i.e., the chiral vibration is near harmonic for a longer spin range. The additional quasiproton also leads to an increase in ϑ from $\sim 50°$ to $\sim 70°$. These two effects explain why the $B(E2)$ values for the twin bands are different in ^{134}Pr, but almost the same in ^{135}Nd.

In summary, we have measured electromagnetic transition probabilities for intraband and interband transitions in the two bands in ^{135}Nd that were previously identified as a composite chiral pair. The intraband transition probabilities in the two bands are nearly identical, establishing them as chiral partners. A microscopic calculation based on the combination of TAC with RPA reproduces all experimental observables quite well, substantiating the theoretical interpretation: At the bottom of the bands, the angular momentum vector oscillates perpendicular to the plane spanned by the long and short axes of the triaxial nuclear shape (chiral vibration). These oscillations slow down with increasing angular momentum, resulting in a decreasing energy splitting between the bands and an increase in the interband $B(E2)$ values. The vibration, then, becomes strongly anharmonic, changing into tunneling between well-established left- and right-handed configurations (chiral rotation), the best realization of chirality in nuclei so far.

One of the authors (S. M.) expresses his gratitude to Dr. C. J. Chiara for several helpful discussions on the LINESHAPE codes. This work has been supported in part by the U.S. National Science Foundation (Grants No. PHY04-57120 and No. INT-0111536); by the Department of Science and Technology, Government of India (Grant No. DST-NSF/RPO-017/98); by the U.S. Department of Energy, Office of Nuclear Physics, under Contracts No. DE-AC02-06CH11357 and No. DE-FG02-95ER40934; and by the University of Notre Dame and the ANL-UND Nuclear Theory Initiative.

[1] S. Frauendorf, Rev. Mod. Phys. **73**, 463 (2001).
[2] S. Frauendorf and J. Meng, Nucl. Phys. A **617**, 131 (1997).
[3] C. M. Petrache *et al.*, Nucl. Phys. A **597**, 106 (1996).
[4] K. Starosta *et al.*, Phys. Rev. Lett. **86**, 971 (2001).
[5] A. A. Hecht *et al.*, Phys. Rev. C **63**, 051302 (2001).
[6] T. Koike *et al.*, Phys. Rev. C **63**, 061304(R) (2001).
[7] D. J. Hartley *et al.*, Phys. Rev. C **64**, 031304(R) (2001).
[8] S. Zhu *et al.*, Phys. Rev. Lett. **91**, 132501 (2003).
[9] C. Vaman *et al.*, Phys. Rev. Lett. **92**, 032501 (2004).
[10] P. Joshi *et al.*, Phys. Lett. B **595**, 135 (2004).
[11] J. Timar *et al.*, Phys. Lett. B **598**, 178 (2004).
[12] E. Grodner *et al.*, Phys. Rev. Lett. **97**, 172501 (2006).
[13] D. Tonev *et al.*, Phys. Rev. Lett. **96**, 052501 (2006).
[14] C. M. Petrache *et al.*, Phys. Rev. Lett. **96**, 112502 (2006).
[15] I.-Y. Lee, Nucl. Phys. A **520**, c641 (1990).
[16] W. F. Piel *et al.*, Phys. Rev. C **35**, 959 (1987).
[17] E. M. Beck *et al.*, Phys. Rev. Lett. **58**, 2182 (1987).
[18] M. Cromaz *et al.*, Nucl. Instrum. Methods Phys. Res., Sect. A **462**, 519 (2001).
[19] K. Starosta *et al.*, Nucl. Instrum. Methods Phys. Res., Sect. A **515**, 771 (2003).
[20] J. Wells and N. Johnson, Oak Ridge National Laboratory Report No. ORNL-6689, p. 44, 1991.
[21] J. F. Ziegler, J. P. Biersack, and U. Littmark, *The Stopping and Range of Ions in Solids* (Pergamon, New York, 1985).
[22] C. Chiara *et al.*, Phys. Rev. C **61**, 034318 (2000).
[23] C. Chiara *et al.*, Phys. Rev. C **64**, 054314 (2001).
[24] N. Johnson *et al.*, Phys. Rev. C **55**, 652 (1997).
[25] T. Koike *et al.*, Phys. Rev. Lett. **93**, 172502 (2004).
[26] V. I. Dimitrov, S. Frauendorf, and F. Dönau, Phys. Rev. Lett. **84**, 5732 (2000).
[27] R. A. Bark *et al.*, Nucl. Phys. A **691**, 577 (2001).
[28] K. Starosta *et al.*, Phys. Rev. C **65**, 044328 (2002).
[29] S. Frauendorf, Nucl. Phys. A **677**, 115 (2000).
[30] M. Baranger and K. Kumar, Nucl. Phys. A **110**, 490 (1968).
[31] P. Ring and P. Schuck, *The Nuclear Many Body Problem* (Springer-Verlag, Berlin, 2004).
[32] D. Almehed and S. Frauendorf (to be published).